CHINA FOUNDRY Research & Development
Vol. 23 No. 4 July 2026
www.springer.com/41230
https://doi.org/10.1007/s41230-026-4271-x

Effect of heat treatment on microstructure and hardness of as-cast Al-Mg_2Si-Eu alloy

Yin-ling Jin[1, 2], Yan-mei Liu[2], Xing Wang[2], *Rui-run Chen[1], Kun Zhang[2], and Shi-jian Li[2]

1. School of Materials Science and Engineering, Harbin Institute of Technology, Harbin 150001, China

2. Shenyang Aircraft Corporation, Aviation Industry Corporation of China, Shenyang 110850, China

Abstract: To further improve the comprehensive performance of Al-15Mg_2Si-0.1Eu alloy, T6 heat treatment was performed for as-cast Al-15Mg_2Si-0.1Eu alloy. The influence mechanism of solid solution treatment on Mg_2Si phase was revealed. The optimal heat treatment process for Al-15Mg_2Si-0.1Eu alloy is solution treatment at 530 °C for 6 h and subsequently aging treatment at 175 °C for 8 h. A short solid solution time or a low solid solution temperature leads to insufficient dissolution of Mg_2Si. Conversely, when the solid solution time is greater than 6 h or the solid solution temperature is higher than 530 °C, the microstructure exhibits coarsening. With an increase in aging time, GP zone, β" phase, and β' phase form within the matrix, corresponding to the under-aged, peak-aged, and over-aged stages respectively. The Al-15Mg_2Si-0.1Eu alloy reaches its peak-aged state after aging treatment at 175 °C for 8 h, during which a large amount of fine dispersed β" phase precipitates within the matrix. Following this 8 h aging treatment, the alloy reaches its maximum hardness of 106 HV.

Keywords: Al-Mg_2Si-Eu alloy; solid solution; aging treatment; microstructure; hardness

CLC numbers: TG146.21 **Document code:** A **Article ID:** 1672-6421(2026)04-624-07

1 Introduction

Aluminum alloys have been widely used in many fields, especially in the automotive and aerospace industries due to their excellent comprehensive performance and lightweight advantages. By adding different alloying elements, different types of alloys can be formed, which can lead to significant changes in the mechanical properties of the alloys[1-3].

In recent years, researchers have continuously developed and studied lightweight aluminum alloys[4, 5], and found that selecting Mg_2Si as reinforcement to prepare Al-Mg_2Si alloys could produce thermodynamically stable Mg_2Si phases, and the preparation process is simple and convenient. Al-Mg_2Si alloys are considered as promising materials to replace Al-Si alloys[6]. However, the Mg_2Si phase formed during the solidification process of Al-Mg_2Si alloy is an intermetallic compound that exhibits strong directional growth, resulting in low comprehensive mechanical properties[7]. This makes it difficult to prepare as-cast Al-Mg_2Si alloys that meet the service requirements, especially the strength.

To further improve the strength and hardness properties of Al-Mg_2Si alloys, it is necessary to further regulate the microstructure by heat treatment, a highly effective method for improving the properties of aluminum alloys[8, 9]. Khorshidi et al.[10] performed solid solution treatment on Al-15Mg_2Si alloy modified with 0.1% Na at 480 °C, 500 °C, and 520 °C for 4 h. Nasiri et al.[11] studied the effect of solid solution treatment at 500 °C for 4 h on the microstructures and mechanical properties of Al-15Mg_2Si alloy modified with P element. Tang et al.[12] investigated heat treatment of Be-modified Al-15Mg_2Si-8Si alloy, with solution treatment temperature of 550 °C followed by aging at 200 °C. However, results mentioned above revealed that elongation of heat-treated Al-Mg_2Si alloy was typically below 5%, with some even falling below 1%. Although heat treatment can significantly improve the strength of Al-Mg_2Si alloy, substantial reduction in ductility results in poor comprehensive tensile properties. This limitation severely restricts the practical application of heat treatment for Al-Mg_2Si alloys[13, 14].

In previous research, it was found that the addition of 0.1wt.% Eu into Al-15Mg_2Si alloy presents good

***Rui-run Chen**

Ph. D., Professor, Doctoral Supervisor. He is a recipient of the National Science Fund for Distinguished Young Scholars, and one of the leading talents of the scientific and technological innovation of the "Ten-thousand Talents Program".

E-mail: ruirunchen@hit.edu.cn

Received: 2024-12-04; Revised: 2025-03-03; Accepted: 2025-03-26

modification effect on both primary and eutectic Mg_2Si[15]. Therefore, this study chooses Al-15wt.% Mg_2Si-0.1wt.% Eu alloy as the basis for further exploring the heat treatment process. The aim is to further optimize the heat treatment process, thereby improving the comprehensive performance of the alloy. This research not only provides reference for formulation of heat treatment process but also lays a foundation for further application of Al-Mg_2Si alloy.

2 Experimental procedures

A resistance furnace was employ for T6 heat treatment of Al-15wt.%Mg_2Si-0.1wt.%Eu alloy (for short Al-15Mg_2Si-0.1Eu, unless otherwise specified, % mentioned in the following text refers to mass percentage, wt.%, and the alloy preparation method is described in the Ref. [15]). The differential scanning calorimetry (DSC) was carried out from 400 °C to 650 °C with heating and cooling rate of 10 °C·min^{-1} under argon gas. Figure 1 shows the DSC curve of Al-15Mg_2Si-0.1Eu alloy during the heating process. It can be seen that the alloy exhibits an endothermic peak at 560 °C. Since the eutectic structure melts first during the heating process of alloy, the upper limit of the solid solution temperature is preliminarily set at 550 °C to prevent the overburning of the microstructure during the heat treatment process. Thus, the solid solution temperatures selected was 490 °C, 510 °C, 530 °C, and 550 °C followed by water quenching, and the solid solution times were 2 h, 4 h, 6 h, 8 h, and 10 h, respectively. The following aging process was conducted at 175 °C for 2 h, 4 h, 6 h, 8 h, 10 h, and 12 h after the optimum solution treatment.

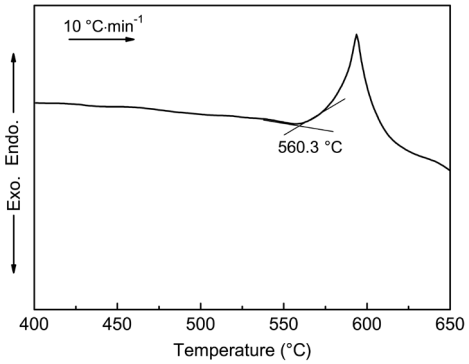

Fig. 1: DSC curve of Al-15Mg_2Si-0.1Eu alloy

Quanta 200FEG field emission scanning electron microscope (SEM) and Talos F200X transmission electron microscope (TEM) both from FEI company were used to analyze and observe the microstructure of Al-Mg_2Si-Eu alloy. The Vickers hardness of the Al-Mg_2Si-Eu alloy was measured using a Vickers hardness tester, applying a load of 1.96 N with a loading time of 10 s. At least 10 tests were conducted, and the average result was recorded. The size, volume fraction, and lattice constant of precipitates were measured using the Image-Pro Plus (IPP) software. A total of 200 precipitates were measured, and the average value was recorded.

3 Results

3.1 Effect of solution treatment temperature on microstructures

Figure 2 shows the SEM images of primary and eutectic Mg_2Si in Al-15Mg_2Si-0.1Eu alloy after solid solution treatment at different temperatures for 6 h. When solution treated at 490 °C, the relatively low solution temperature induces an tendency for corner rounding of primary Mg_2Si. As the solid solution temperature increases, the sharp corners of the primary Mg_2Si particles become rounded. When the temperature increases to 530 °C, the sharp corners of the primary Mg_2Si phase are noticeably smoother, and the size of the primary phase decreases. Further increasing the temperature to 550 °C, although the sharp corners continue to become more rounded, the size of the primary Mg_2Si phase increases again. For eutectic Mg_2Si, partial dissolution occurs at thinner regions when solution-treated at 490 °C. With rising temperature,

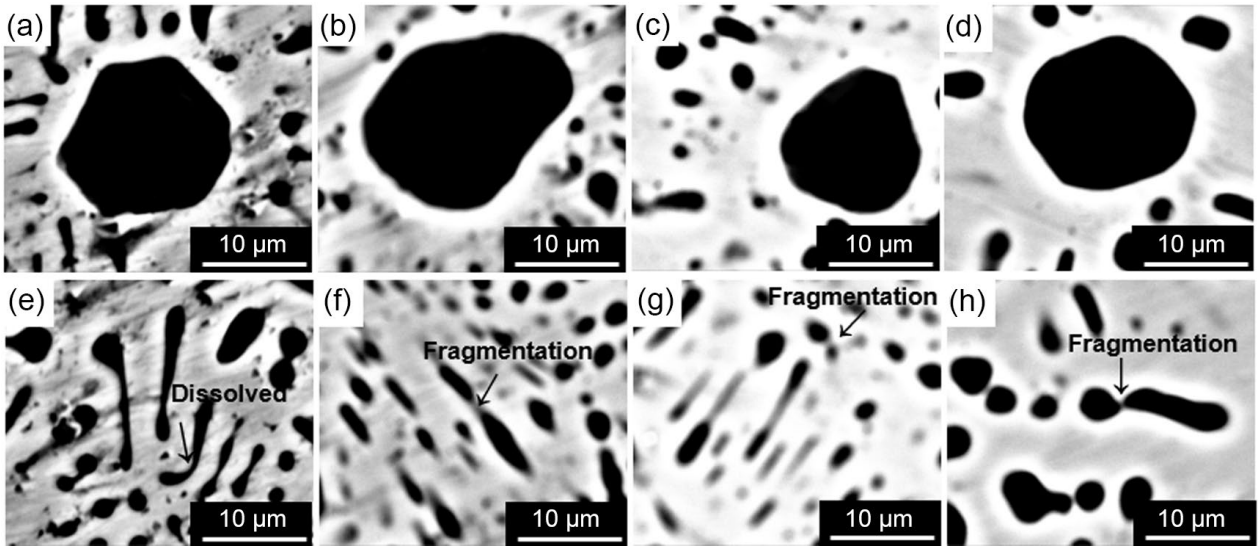

Fig. 2: SEM images of Al-15Mg_2Si-0.1Eu alloy solution treated at different temperatures for 6 h: (a) and (e) 490 °C; (b) and (f) 510 °C; (c) and (g) 530 °C; (d) and (h) 550 °C; (a) to (d) primary Mg_2Si; (e) to (h) eutectic Mg_2Si

fragmentation of eutectic Mg_2Si initiates. At 530 °C, the long fibrous eutectic Mg_2Si fragments into short rod-like particles with edge spheroidization. When further increases to 550 °C, fragmented rod-eutectic Mg_2Si undergoes coarsening.

In summary, with the increase of solid solution temperatures, the trend of round and spheroidization of the sharp corners of primary Mg_2Si and dissolution of eutectic Mg_2Si increases. The solid solution temperature of 530 °C exhibits the most effective rounding of primary Mg_2Si and greastest dissolution of eutectic Mg_2Si. When the solid solution temperature below 530 °C, eutectic Mg_2Si does not dissolve sufficiently; When the solid solution temperature increases to 550 °C, the primary and eutectic Mg_2Si structures undergo coarsening, which is detrimental. Therefore, solid solution temperature of 530 °C was selected for further research on the solid solution time.

3.2 Effect of solution treatment time on microstructures

Figure 3 illustrates the microstructure of the primary Mg_2Si phase in Al-15Mg_2Si-0.1Eu alloy solution-treated at 530 °C for varying durations. Prolonged solution time exhibits comparable effects with increasing temperature in promoting corner rounding of primary Mg_2Si. When the solid solution time is 2 h, the sharp corners of primary Mg_2Si begin to undergo rounding. After increasing the solid solution time to 4 h, progressive corner rounding continues. The optimal combined effect of rounding and refinement of primary Mg_2Si sharp corners is achieved with a solution treatment time of 6 h. Further extension to 8 h, the primary Mg_2Si shows a trend of coarsening. Increasing the solid solution time to 10 h, the coarsening phenomenon of primary Mg_2Si is more obvious. Consequently, the optimum solution treatment parameters for Al-15Mg_2Si-0.1Eu alloy are determined to be at 530 °C for 6 h.

The results of Figs. 2 and 3 show that increasing the solution treatment time has a similar effect as raising the solution temperature, both increasing the rounding tendency of sharp primary Mg_2Si. But beyond a certain value, coarsening occurs. The Mg and Si atoms in both the primary and eutectic Mg_2Si are solid dissolved in the α-Al matrix during the solution of the alloy. The choice of solution temperature and time is generally aimed at maximizing the dissolution of second phases, while preventing the structure for coarsening. The best solution treatment process is determined to 530 °C/6 h.

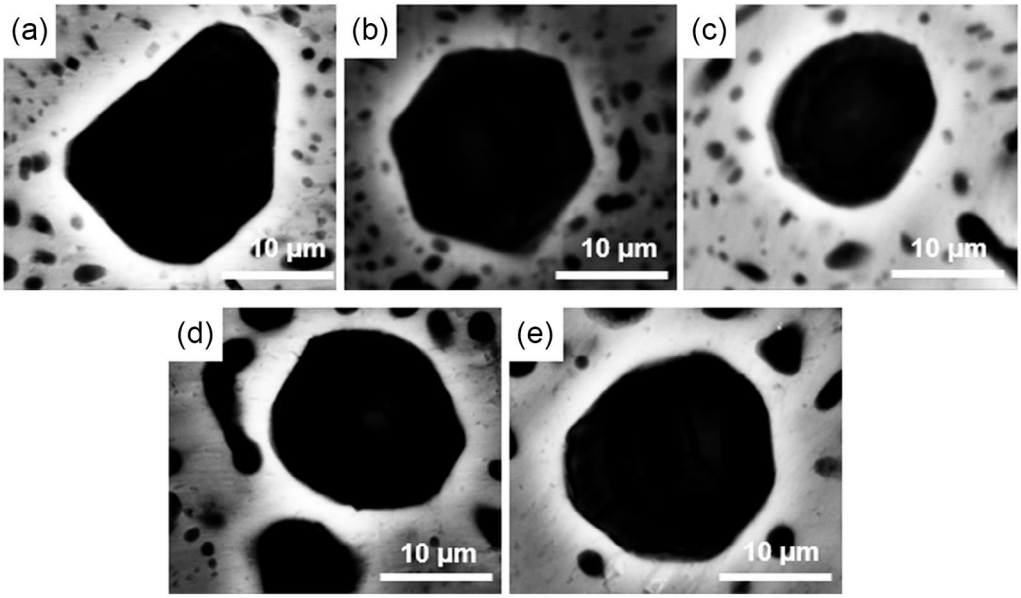

Fig. 3: SEM images of Al-15Mg_2Si-0.1Eu alloy solution treated at 530 °C for different solution times: (a) 2 h; (b) 4 h; (c) 6 h; (d) 8 h; (e) 10 h

3.3 Effect of aging time on hardness of Al-15Mg_2Si-0.1Eu alloy

The Al-15Mg_2Si-0.1Eu alloy which solution treated at 530 °C/6 h and followed by water quenching was subjected to different aging treatments at 175 °C. The effect of different aging times on hardness of Al-15Mg_2Si-0.1Eu alloy was studied. Figure 4 shows the Vickers hardness variation curve of Al-15Mg_2Si-0.1Eu alloy under different aging times. As the aging time increases, the hardness of the alloy increases firstly and then decreases. After 8 h aging treatment, the alloy reaches its peak hardness of 106 HV. Subsequently, by further increasing the aging time, the hardness of the alloy

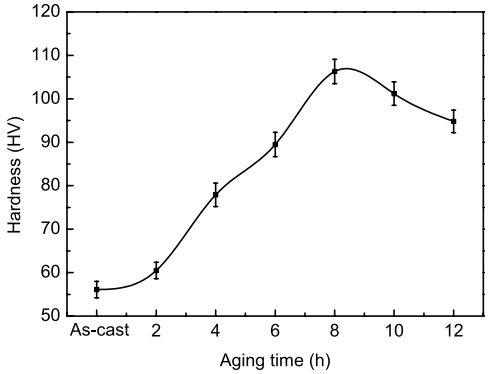

Fig. 4: Hardness curve of Al-15Mg_2Si-0.1Eu alloy with different aging times

begins to decline. According to the hardness curve, the aging process of Al-15Mg_2Si-0.1Eu alloy can be divided into three stages: under-aged (2–8 h), peak-aged (8 h), and over-aged (8–12 h).

Other researchers have also obtained similar results. Khorshidi[10] heat treated Al-15Mg_2Si-0.1Na alloy at different temperatures for 4 h, and the best solution treatment temperature obtained was 500 °C. Malekan et al.[16] found that the best solution treatment temperature for Al-15Mg_2Si alloy for 4 h holding time was 550 °C. Li et al.[13] found Al-15%Mg_2Si alloy reached a peak hardness of 85 HV after solution treatment at 520 °C for 6 h and ageing for 10 h. Sun et al.[17] found that Al-15%Mg_2Si alloy, when solution treated at 550 °C followed by aging at 200 °C, achieved a hardness of 95 HV, whereas the Al-15Mg_2Si-1Cu alloy exhibited a hardness of 144 HV.

3.4 Effect of aging time on microstructures of Al-15Mg_2Si-0.1Eu alloy

In order to investigate the effect of different aging times on microstructure of Al-15Mg_2Si-0.1Eu alloy, TEM was performed on the microstructure during under-aged (2 h), peak-aged (8 h), and over-aged (10 h) stages.

Figure 5 shows the TEM microstructure of Al-15Mg_2Si-0.1Eu alloy during under-aged stage. It can be observed that there are many point precipitates and some needle precipitates in the matrix, as indicated by arrows in Fig. 5(a). From high resolution TEM (HRTEM), as shown in Fig. 5(b), it can be seen there are some areas with deeper contrast in the matrix. Performing inverse Fourier transform (IFFT) on Regions A and B in Fig. 5(b), as shown in Fig. 5(c) and Fig. 5(d), lattice distortion exists in these regions. The size of the dot shaped precipitates in Fig. 5(a) was measured using IPP software, and the average diameter of the dot shaped precipitates is 2.2 nm, and the average length of the needle shaped precipitates is approximately 21.1 nm. According to Vissers et al.[18], GP zone is formed in the early stage of aging of Al-Mg-Si alloy, consisting of spherical particles with a size of 1–3 nm or needle shaped particles with a size of 2 nm×2 nm×20 nm, which is similar to this study. Therefore, it is believed that GP zone exhibits in the matrix during the early stage of aging.

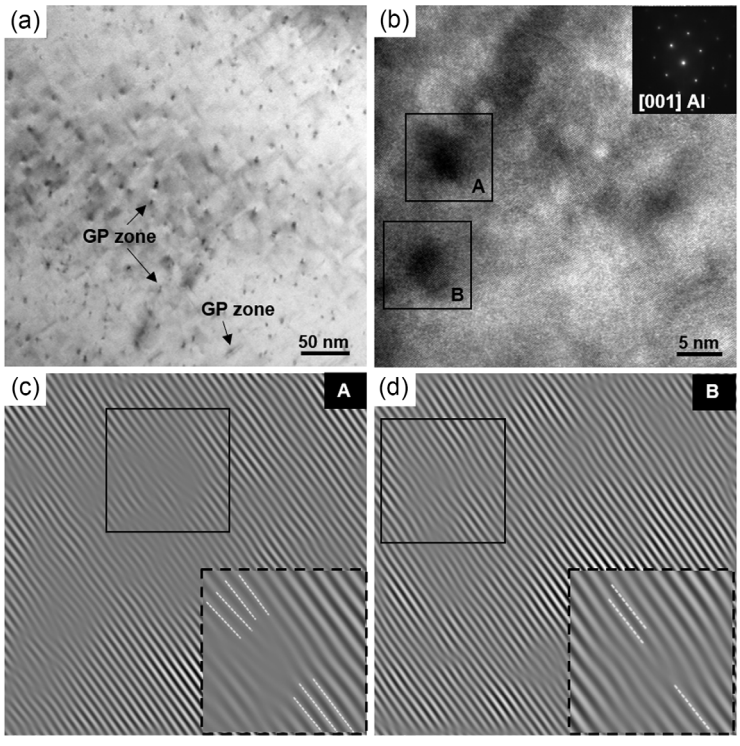

Fig. 5: TEM analysis for under-aged Al-15Mg_2Si-0.1Eu alloy (a–d)

Figure 6 presents the TEM microstructure of the peak-aged alloy, revealing a large number of fine dispersed precipitation phases in the matrix. The HRTEM was conducted in another paper[15], and lattice constants a=1.514 nm, c=0.673 nm, and angle of 105° were obtained. The average diameter of the disc-shaped precipitation phase is 4.12 nm, which is measured using IPP software. According to Zandbergen et al.[19], the β" precipitate has a monoclinic structure, space group C2/m, lattice constants a=1.516 nm, c=0.674 nm, and an angle of 105.3°, and the size of β" is 4 nm. The lattice constants and sizes of the precipitated phases in the peak-aged stage measured in this study are not significantly different from the reported results in Ref. [19]. As the most important strengthening precipitated phase in Al-Mg-Si alloys, the high-density dispersion of β" precipitates directly accounts for the peak hardness.

Figure 7 shows the TEM structure of the precipitated phase in the Al-15Mg_2Si-0.1Eu alloy with over-aged. There are still many precipitated phases in the matrix, but under 10 h aging treatment, some precipitated phases grows, and their size is larger than that of β" precipitated phase in the peak-aged stage. Figures 7(b) and (c) show high-resolution images and enlarged images of the precipitated phase. According to Fig. 7(c), the lattice constant of the precipitated phase measured during the over-aged stage is a=0.719 nm. The average diameter of the grown precipitated phase, measured by IPP software, is about 9.41 nm. According to Ding et al.[20], the lattice constant of β' precipitate phase in the over-aged stage is a=0.715 nm, with a diameter of approximately 10 nm. Therefore, it is believed that under 10 h aging treatment, some β"

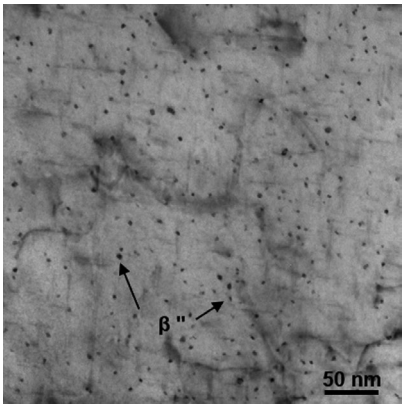

Fig. 6: TEM analysis for peak-aged Al-15Mg_2Si-0.1Eu alloy

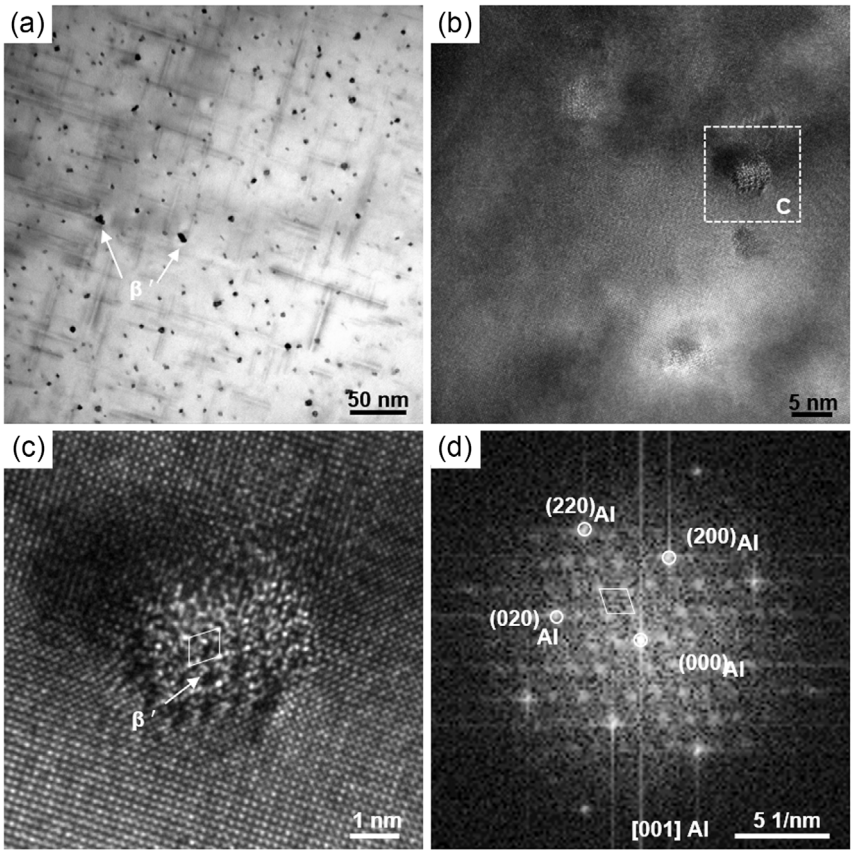

Fig. 7: TEM analysis for over-aged Al-15Mg_2Si-0.1Eu alloy: (a) bright-field image; (b) high-resolution image of precipitated phase; (c) enlarged image of precipitated phase; (d) fourier transform image

precipitates in the matrix grow into β'. The hardness of the Al-15Mg_2Si-0.1Eu alloy decreases when transitioning from the peak-aged state to the over-aged state.

The average diameter and volume fraction of precipitates in Al-15Mg_2Si-0.1Eu alloy during under-aged, peak-aged, and over-aged stages were statistically analyzed using IPP software. Approximately 200 precipitates were measured and averaged, and the results are shown in Fig. 8. The average diameter counted during over-aged stage is for the β' phase, and the volume fraction during over-aged stage is for all precipitated phases in the matrix. It can be observed that as the aging time increases, the diameter and volume fraction of the precipitated phase also increase. In the early stage of aging, the size and volume fraction of the GP zone are relatively small. The number of GP zone depends on the concentration of vacancies in the matrix after quenching. These vacancies enable the enrichment and diffusion of and Mg and Si solute atoms. The more vacancies there are, the easier for Mg and Si atoms to be enriched and migrated. As the aging time increases, the diameter and volume fraction of β" in the peak-aged stage are larger than those in the GP zones, and the distribution of β" is dispersed. Continue to increase the aging time, to reach over-aged stage, some β" precipitates begin to grow into the β', with a diameter larger than that of β" in the peak-aged stage.

4 Discussion

Heat treatment is the process of heating Al-Mg_2Si-Eu alloy to a certain temperature and holding for a period of time, allowing the strengthening solute elements Mg and Si to fully dissolve into α-Al matrix, followed by quenching to form a

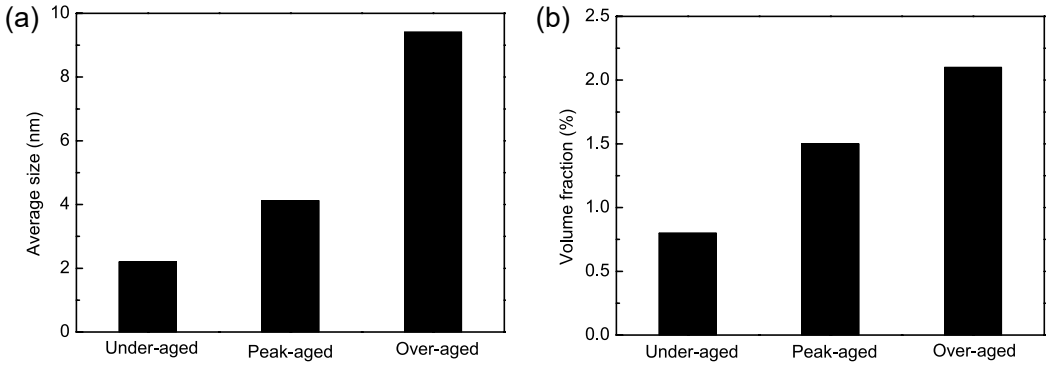

Fig. 8: Mean diameter (a) and volume fraction (b) of precipitates at different aging stages

supersaturated solid solution. The essence of solid solution of Al-Mg_2Si alloy is the diffusion of alloying elements in the matrix, which Mg and Si in Mg_2Si crystals diffuse into the α-Al matrix as solute atoms. In order to further analyze the dissolution behavior and size changes of Mg_2Si during the solid solution process, dissolution kinetics model for individual Mg_2Si particles is established. The solute diffusion in α-Al matrix can be expressed by the classical diffusion equation[21]:

$$\frac{\partial C(r,t)}{\partial t} = D\nabla_2 C(r,t) \tag{1}$$

where $C(r,t)$ – solute composition at different position and time (mol·L^{-1});

t – dissolution time (s);

D – diffusion coefficient (m^2·s^{-1}).

During isothermal solid solution treatment, the diffusion coefficient D is considered a constant. During particle dissolution, solute conservation occurs at the interface, which can be expressed as:

$$\left(C_\beta - C_\alpha\right)\frac{\mathrm{d}R}{\mathrm{d}t} = D\frac{\partial C}{\partial R}\Big|_{r=R} \tag{2}$$

where C_α – solute concentration at the interface between particle and matrix (mol·L^{-1});

C_β – solute concentration in particle (mol·L^{-1});

R – radius of dissolved particles (m).

The approximate solution of the above equation can be expressed as[21]:

$$\frac{\mathrm{d}R}{\mathrm{d}t} = -\frac{k}{2}\left(\frac{D}{R} + \sqrt{\frac{D}{\pi t}}\right) \tag{3}$$

Among them, k can be represented as:

$$k = \frac{2\left(C_\alpha - C_\mathrm{m}\right)}{\left(C_\beta - C_\alpha\right)} \tag{4}$$

where C_m – solute concentration in the matrix (mol·L^{-1}).

During the dissolution process of a single particle, the decrease in particle size can be used to represent the amount of particle dissolution. The decrease in particle size R_d and the particle dissolution rate can be expressed as:

$$R_\mathrm{d} = R_0 - R \tag{5}$$

$$\frac{\mathrm{d}R_\mathrm{d}}{\mathrm{d}t} = \frac{KD}{2\left(R_0 - R_\mathrm{d}\right)} + \frac{k}{2}\sqrt{\frac{D}{\pi t}} \tag{6}$$

where R_d – particle size reduction (m);

R_0 – initial particle size (m);

$\frac{\mathrm{d}R_\mathrm{d}}{\mathrm{d}t}$ – particle dissolution rate (m·s^{-1}).

According to the Gibbs-Thomson equation, the atomic concentration at the interface between the second phase particles with a curvature radius r and the matrix can be expressed as[22]:

$$C_\alpha(r) = C_\alpha(\infty)\exp\left(\frac{2\gamma V_\mathrm{p}}{rR_\mathrm{c}T}\right) \tag{7}$$

where $C_\alpha(r)$ – atomic concentration at the interface between the second phase and the matrix with a curvature radius of r (mol·L^{-1});

$C_\alpha(\infty)$ – atomic concentration at the interface between the second phase and the matrix at the planar interface (mol·L^{-1});

γ – interfacial energy (J);

V_p – molar volume (L·mol^{-1});

r – curvature radius (m);

R_c – gas molar constant;

T – temperature (K).

Due to the high concentration of Mg and Si atoms in Mg_2Si particles, and the low initial concentration of Mg and Si atoms in α-Al matrix, there is a large concentration gradient. According to Fick's diffusion law, Mg and Si atoms in Mg_2Si particles will diffuse and dissolve. For primary Mg_2Si particles, which morphology is composed of different planes, sharp corners and edges will form between different planes. According to Eqs. (3–7), due to the small curvature radius at the sharp corners of Mg_2Si particles, the concentration of Mg and Si atoms at the interface between Mg_2Si sharp corners and α-Al matrix is very high, and there is a large concentration gradient between Mg and Si atoms in the α-Al matrix. During solution treatment process, as the solution time increases, the Mg and Si atoms at the sharp corners of primary Mg_2Si diffuse from the high concentration zone to the low concentration position firstly, and the sharp corners of primary Mg_2Si dissolve, resulting in the rounding of primary Mg_2Si particles. Furthermore, with Eu modification, the morphology of primary Mg_2Si evolves into a polyhedral shape that closely approaches a tetrahedral geometry, which provides a good prerequisite for the spheroidization of primary Mg_2Si. For eutectic Mg_2Si, the morphology of Mg_2Si is long fibrous[15]. There are defects in the fibrous Mg_2Si structure, and the curvature radius of the defect location is small. As the solid solution progresses, the Mg_2Si dissolves firstly, and in some cases, they even some break into several segments.

When the solid solution time is too long or the temperature is too high, both primary Mg_2Si and eutectic Mg_2Si undergo coarsening. During the long-term solid solution treatment process, the coarsening of Mg_2Si is also controlled by the diffusion process, its coarsening kinetics can be expressed as[23]:

$$d^n - d_0^n = kt \tag{8}$$

where d – grain size after coarsening time t (m);

d_0 – initial grain size (m);

k – coarsening rate constant;

n – coarsening index;

t – coarsening time (s).

According to Ostwald ripening theory, the grain coarsening model can be expressed according to Lifshitdz-Slyozov-Wagner equation modified by Ardell[24]:

$$R^3 - R_0^3 = K_\mathrm{MLSW}t \tag{9}$$

It can be seen that with the increasing of solid solution time, conditions are provided for the coarsening of Mg_2Si, and the size of Mg_2Si increases, leading to the coarsening phenomenon of Mg_2Si. There are two possible reasons for the coarsening of Mg_2Si[24]. One is due to the dissolution of Mg and Si solution atoms in the α-Al matrix at high temperatures and long time, and the diffusion segregation to the Mg_2Si via the matrix, which

results in the coarsening of the Mg_2Si. The other one is that Mg and Si atoms dissolved in the α-Al matrix are easily migrated to the crystal defect sites at high temperatures. As the solution time is extended, the Mg and Si atoms may re-nucleate and grow at the defect sites within the Mg_2Si crystal, embedding themselves into the original Mg_2Si particles and promoting their coarsening.

5 Conclusions

The heat treatment process of Al-15Mg_2Si-0.1Eu alloy was optimized in this study. The effects of heat treatment on the microstructure and hardness of Al-15Mg_2Si-0.1Eu alloy were analyzed. The main conclusions obtained are as follows:

(1) The optimal heat treatment process for Al-15Mg_2Si-0.1Eu alloy is solution treatment at 530 °C/6 h, followed by an aging treatment at 175 °C/8 h. Under these conditions, the Al-15Mg_2Si-0.1Eu alloy reaches its peak hardness of 106 HV.

(2) Short solid solution time or low solid solution temperature leads to Mg_2Si insufficient dissolution. When the solid solution time is greater than 6 h or the solid solution temperature is higher than 530 °C, the microstructures coarsen. After heat treatment, the sharp corners of primary Mg_2Si in Al-15Mg_2Si-0.1Eu alloy undergo rounding and spheroidization and eutectic Mg_2Si undergoes dissolution.

(3) The Al-15Mg_2Si-0.1Eu alloy reaches its peak-aged state after 8 h aging treatment, during which a large amount of fine dispersed β" precipitates in the matrix. With different aging times, GP zone, β" phase, and β' phase are formed in the matrix, corresponding to the under-aged (2–8 h), peak-aged (8 h), and over-aged (8–12 h) stages, respectively.

Acknowledgment

This work was supported by the National Natural Science Foundation of China (No. 52425401).

Conflict of interest

Prof. Rui-run Chen is an EBM of *CHINA FOUNDRY*. He was not involved in the peer-review or handling of the manuscript. The authors have no other competing interests to disclose.

References

[1] Qiu Y Q, Wu M W, Qin X P, et al. Phase-field lattice-Boltzmann study on fully coupled thermal-solute-convection dendrite growth of Al-Cu alloy. China Foundry, 2024, 21(2): 125–136.
[2] Xu Y W, Zhan H Y, Tong W, et al. To improve robustness of mechanical properties of semi-solid cast A356 alloy using taguchi design method. China Foundry, 2024, 21(2): 175–184.
[3] Zhu G Q, Wang L, Su B X, et al. Deciphering the microstructural development and excellent ductility in electron beam wire-fed additive manufacturing of Ti-6Al-3Nb-2Zr-1Mo alloys based on high deposition rate. Additive Manufacturing, 2024, 94: 104485.
[4] Gao M Q, Chen Z N, Kang H J, et al. Microstructural characteristics and mechanical behavior of B_4C_p/6061Al composites synthesized at different hot-pressing temperatures. Journal of Materials Science & Technology, 2019, 35(8): 1523–1531.
[5] Jiang W M, Zhu J W, Li G Y, et al. Enhanced mechanical properties of 6082 aluminum alloy via SiC addition combined with squeeze casting. Journal of Materials Science & Technology, 2021, 88: 119–131.
[6] Jiang W Q, Xu X F, Zhao Y G, et al. Effect of the addition of Sr modifier in different conditions on microstructure and mechanical properties of T6 treated Al-Mg_2Si in-situ composite. Materials Science and Engineering: A, 2018, 721: 263–273.
[7] Li A, Zhao X P, Huang H Y, et al. Fine-tuning the ductile-brittle transition temperature of Mg_2Si intermetallic compound via Al doping. International Journal of Minerals, Metallurgy, and Materials, 2019, 26(4): 507–515.
[8] Liu Z Q, Zhou J, Yang L, et al. Study on microstructure and properties of Mg-Al-Si-Ca alloy by heat treatment. Journal of Alloys and Compounds, 2023, 947: 169431.
[9] Cai Q, Mendis C L, Wang S H, et al. Effect of heat treatment on microstructure and tensile properties of die-cast Al-Cu-Si-Mg alloys. Journal of Alloys and Compounds, 2021, 881: 160559.
[10] Khorshidi R, Honarbakhsh Raouf A, Emamy M, et al. The evolution of heat treatment on the tensile properties of Na-modified Al-Mg_2Si in situ composite. Advanced Materials Research, 2011, 311–313: 283–286.
[11] Nasiri N, Emamy M, Malekan A, et al. Microstructure and tensile properties of cast Al-15Mg_2Si composite: Effects of phosphorous addition and heat treatment. Materials Science and Engineering: A, 2012, 556: 446–453.
[12] Tang P, Yu F Y, Teng X D, et al. Effect of beryllium addition and heat treatment on the microstructure and mechanical properties of the 15%Mg_2Si/Al-8Si composite. Materials Characterization, 2021, 180: 111416.
[13] Li M R, Sun Y L, Li C, et al. Effect of Cu addition on precipitation and age-hardening response of an Al-15Mg_2Si alloy. Materials Characterization, 2020, 169: 110611.
[14] Li Z D, Li C, Liu Y C, et al. Effect of heat treatment on microstructure and mechanical property of Al-10%Mg_2Si alloy. Journal of Alloys and Compounds, 2016, 663: 16–19.
[15] Jin Y L, Fang H Z, Chen R R, et al. Morphological modification of Mg_2Si phase and strengthening mechanism in Mg_2Si/Al composites by Eu addition and T6 heat treatment. Journal of Materials Science & Technology, 2023, 159: 151–162.
[16] Malekan A, Emamy M, Rassizadehghani J, et al. The effect of solution temperature on the microstructure and tensile properties of Al-15Mg_2Si composite. Materials & Design, 2011, 32(5): 2701–2709.
[17] Sun Y L, Hu M, Li M R, et al. The effect of solution temperature on the precipitates evolution and aging hardening response of Al-15%Mg_2Si(–1%Cu) alloys. Journal of Materials Research and Technology, 2022, 17: 1330–1337.
[18] Vissers R, Van Huis M A, Jansen J, et al. The crystal structure of the β′ phase in Al-Mg-Si alloys. Acta Materialia, 2007, 55(11): 3815–3823.
[19] Zandbergen H W, Andersen S J, Jansen J. Structure determination of Mg_5Si_6 particles in Al by dynamic electron diffraction studies. Science, 1997, 277(5330): 1221–1225.
[20] Ding L P, Jia Z H, Nie J F, et al. The structural and compositional evolution of precipitates in Al-Mg-Si-Cu alloy. Acta Materialia, 2018, 145: 437–450.
[21] Zuo Q, Liu F, Wang L, et al. An analytical model for secondary phase dissolution kinetics. Journal of Materials Science, 2014, 49(8): 3066–3079.
[22] Yu H C, Wang H Y, Chen L, et al. Spheroidization of primary Mg_2Si in Al-20Mg_2Si-4.5Cu alloy modified with Ca and Sb during T6 heat treatment process. Materials Science and Engineering: A, 2017, 685: 31–38.
[23] Svoboda J, Zickler G A, Kozeschnik E, et al. Generalization of classical Hillert's grain growth and LSW theories to a wide family of kinetic evolution equations and stationary distribution functions. Acta Materialia, 2022, 235: 118085.
[24] Ardell A J. On the coarsening of grain boundary precipitates. Acta Metallurgica, 1972, 20: 601–609.